Computers and Chemical Engineering 100 (2017) 104–118

Contents lists available at ScienceDirect

Computers and Chemical Engineering

journal homepage: www.elsevier.com/locate/compchemeng

# Modeling and simulation of forward osmosis process using agent-based model system

Mostafa Taherian, Seyed Mahmoud Mousavi*

*Chemical Engineering Department, Faculty of Engineering, Ferdowsi University of Mashhad, Mashhad, Iran*

ARTICLE INFO

*Article history:*
Received 29 August 2016
Received in revised form 2 January 2017
Accepted 4 February 2017
Available online 7 February 2017

*Keywords:*
Agent-based model
Forward osmosis
FO mode
NetLogo
Simulation

ABSTRACT

In recent years forward osmosis (FO) process has attracted considerable attention in the field of water treatment and desalination. However, the lack of sufficient information on all possible parameters, affecting the process performance, is a major obstacle that avoids improving the function of this method. In this study, an algorithm based upon a reliable model was developed for osmosis through asymmetric membrane oriented in FO mode to be applied in agent-based model. This model was built in the NetLogo platform, which is a programmable modeling environment for simulating natural phenomena. The feasibility of this modeling was proven by comparing the simulation results and empirical data obtained from literature. The influence of net bulk osmotic pressure difference between the draw solution (DS) and the feed solution (FS) on average water flux was studied for various draw solutes. Furthermore, the effects of process parameters, including temperature, length of module, FS cross-flow velocity, pure water permeability coefficient, and structural parameter of membrane on average water flux were investigated. As a result, it could be concluded that Netlogo agent-based model had the quite well potential to simulate the FO process.



## 1. Introduction

Due to scarcity of global water resources and growing demands of population (Alnouri et al., 2016; Elimelech, 2006; Mahmoodi et al., 2016; UNESCO, 2011), several technologies especially membrane processes have been evaluated to provide clean water (Borsi and Lorain, 2012; Lutchmiah et al., 2014; Soni et al., 2009). Amongst these processes used to desalinate aqueous solutions, forward osmosis (FO) has found special position in the last few decades. It is due to the features such as less operation energy requirement (Chung et al., 2012), high water recovery (McCutcheon et al., 2005), and less tendency to fouling (Achilli et al., 2009; Kumar and Pal, 2015; Lutchmiah et al., 2014). Therefore, FO technology is now applied to diverse fields (Jiao et al., 2004; Lutchmiah et al., 2014; McCutcheon et al., 2006; Pardeshi et al., 2016; Thorsen and Holt, 2009; Yang et al., 2009).

The FO process utilizes the osmosis phenomenon for transport of water across a selectively semi-permeable membrane from a high water chemical potential solution (feed solution or FS) to a low water chemical potential solution (draw solution or DS). In fact, this process proceeds spontaneously with inherent osmotic pressure difference driving force between the FS and DS (Cath et al., 2006). The membrane which is usually used in this process is asymmetric in design. This leads to the occurrence of two common modes depending on its orientation. One of them is FO mode (FS facing the active layer of membrane and DS facing the porous support layer) and the other is PRO mode (DS facing the active layer of membrane and FS facing the porous support layer) (McCutcheon and Elimelech, 2006).

The presence of concentration polarization (CP) which is known as one of the primary difficulties to use FO technology (Dabaghian and Rahimpour, 2015; McCutcheon and Elimelech, 2006) led to non-linearity of this process (Phuntsho et al., 2014). Furthermore, the FO process performance depends upon multiple agents, including the solution characteristics (such as solute type, concentration, and volume of FS and DS), the operational parameters (such as temperature and cross-flow velocity), the membrane characteristics (such as type, area, orientation, and structure of the membrane), and module dimensions (Pardeshi et al., 2016; Phuntsho et al., 2012; Shim and Kim, 2013). These lead to the complexity of the FO process.

On the other hand, the FO process modeling allows researchers to predict water flux of the process without actually conducting a physical experiment. There have been pervious publications on the modeling of FO (McCutcheon and Elimelech, 2006, 2007; Tan and Ng, 2008; Tang et al., 2010). Moreover, various modeling techniques including the numerical simulation (Jung et al., 2011; Shim and Kim, 2013), computational fluid dynamic (CFD) (Gruber et al., 2011), and

* Corresponding author.
*E-mail address:* mmousavi@um.ac.ir (S.M. Mousavi).

http://dx.doi.org/10.1016/j.compchemeng.2017.02.005
0098-1354/

**Nomenclature**

| | |
|---|---|
| $A$ | Pure water permeability coefficient (m/Pa s) |
| $a$ | Effective membrane area ($m^2$) |
| $C_0$ | Initial solute concentration of solution (mol/l) |
| $D$ | Diffusion coefficient ($m^2$/s) |
| $d_h$ | Hydraulic diameter (m) |
| $H$ | Channel height (m) |
| $J_{water}$ | Water flux (l/$m^2$ h or μm/s) |
| $K$ | Solute resistivity for diffusion within the membrane support layer (s/m) |
| $k$ | Mass transfer coefficient (m/s) |
| $L$ | Channel length (m) |
| $MW_{water}$ | Molecular weight of water (g/mol) |
| $Re$ | Reynolds number |
| $S$ | Structural parameter of the membrane support layer (m) |
| $Sc$ | Schmidt number |
| $Sh$ | Sherwood number |
| $T$ | Temperature (K) |
| $t$ | Thickness of the membrane support layer (m) |
| $\Delta t$ | Tick interval (s) defined by Eq. (9) |
| $V_0$ | Initial volume of solution (l) |
| $\%V_{water}$ | Volumetric fraction of water in solution |
| $v$ | Cross-flow velocity (m/s) |
| $W$ | Channel width (m) |
| $x_{water}$ | Weight fraction of water in solution |

*Greek symbols*

| | |
|---|---|
| $\varepsilon$ | Porosity of the membrane support layer |
| $\mu$ | Dynamic viscosity (Pa s) |
| $\pi$ | Osmotic pressure (Pa) |
| $\rho$ | Density (kg/$m^3$) |
| $\tau$ | Tortuosity of the membrane support layer |

*Subscripts*

| | |
|---|---|
| $b$ | At bulk solution |
| $D$ | Draw solution |
| $eff$ | Effective |
| $F$ | Feed solution |
| $m$ | At membrane |

finite elements method (FEM) (Li et al., 2011; Sagiv and Semiat, 2011) have been applied to examine the CP phenomenon in FO process. In a recent study, Gruber et al. (2016) demonstrated how a CFD model can be applied to examine the way in which different geometry and flow parameters influence module performance. Deshmukh et al. (2015) modeled the potential performance of a FO unit operation and evaluated the impact of membrane transport properties on process performance. However, the lack of comprehensive analysis poses a very important problem in terms of utilizing the FO process for future development and commercialization. Therefore, there is a need to develop a more robust model and simulation which provides a better understanding of the performance of FO.

In recent decades agent-based modeling and simulation has been introduced as an almost new method for modeling of a complex phenomenon (Bonabeau, 2002; Macal and North, 2010). This model is a kind of computational simulation that has appeared to survey complex systems. It is continued to increase in significance and popularity as a powerful tool for simulating social and natural phenomena (Macal and North, 2010). Recently, agent-based modeling has been applied in diverse application areas, including economy (Damaceanu, 2008), ecology (Grosman et al., 2011), energy analysis (Van Dam et al., 2008), medicine (Mansury and Deisboeck, 2004), and biology (Paton et al., 2004). However, there are few published researches using it in the field of process modeling (Eo et al., 2000; Katare and Venkatasubramanian, 2001; Pogson et al., 2006).

Amongst various software platforms for scientific agent-based models, NetLogo is a high-level environment. It provides a user-friendly environment, a large-collection of pre-written models in its model-library, two and three-dimensional modeling world view, visualization abilities, and easy-to-use application with simple programmable modeling platform for simulating natural phenomena (Railsback et al., 2006; Wilensky, 1999). NetLogo was designed by Uri Wilensky in 1999 (Wilensky, 1999).

In the present study, an agent-based model of osmosis through asymmetric membrane oriented in FO mode was developed for the first time using the NetLogo platform. The aim of this study was to examine the feasibility of using an agent-based model to simulate and provide a robust tool for simulation of FO process. This model would be able to predict the process performance under different applied scenarios. For this purpose, firstly an algorithm was developed which is applicable in this model. Then, it was applied in the NetLogo environment for FO process simulation. According to this NetLogo platform and collected data library in it, the water flux of FO process and changes in process parameters can be evaluated with a minimum of spending time. Furthermore, the effects of process parameters on the simulation outputs were examined. Experimental water flux data obtained from the use of deionized (DI) water and brackish water (BW) as FS under specific conditions were used for model validation.

## 2. Modeling and simulation

### 2.1. Agent-based model

Agent-based modeling offers a promising approach to deal with complex systems based upon agents (Bonabeau, 2002). An agent-based model typically comprises of three factors including agents, agent relationships, and agent's environment (Macal and North, 2010). In agent-based modeling, systems are modeled by a series of autonomous and interacting entities called agents (Bonabeau, 2002). Agents can perceive their environment and interact with each other and with the model's world by a set of pre-defined goals (Macal and North, 2010).

In the NetLogo platform, the world view in the Interface tab can be made up of agents which are two of types: patches or stationary agents and turtles or mobile agents. Turtles are agents that interact with each other and move around in the grid spaces called patches (Railsback et al., 2006; Wilensky, 1999).

### 2.2. Application procedure using NetLogo

The procedure applied in the Netlogo simulator comprises the following main parts (Railsback et al., 2006; Wilensky, 1999):

- The definition of global variable and design of algorithm.
- "Setup procedure" to start the simulation.
- "Go procedure" which is run continuously by the system.

In the code tab of NetLogo platform, the codes related to the planned algorithm (including the definition of variables, designing the simulator environment, and calculating the outputs) should be written. The process can be controlled using buttons provided on the simulator environment. "Setup" initializes the model and "Go" makes it run. Then, the outputs of the model are obtained by the planned algorithm.

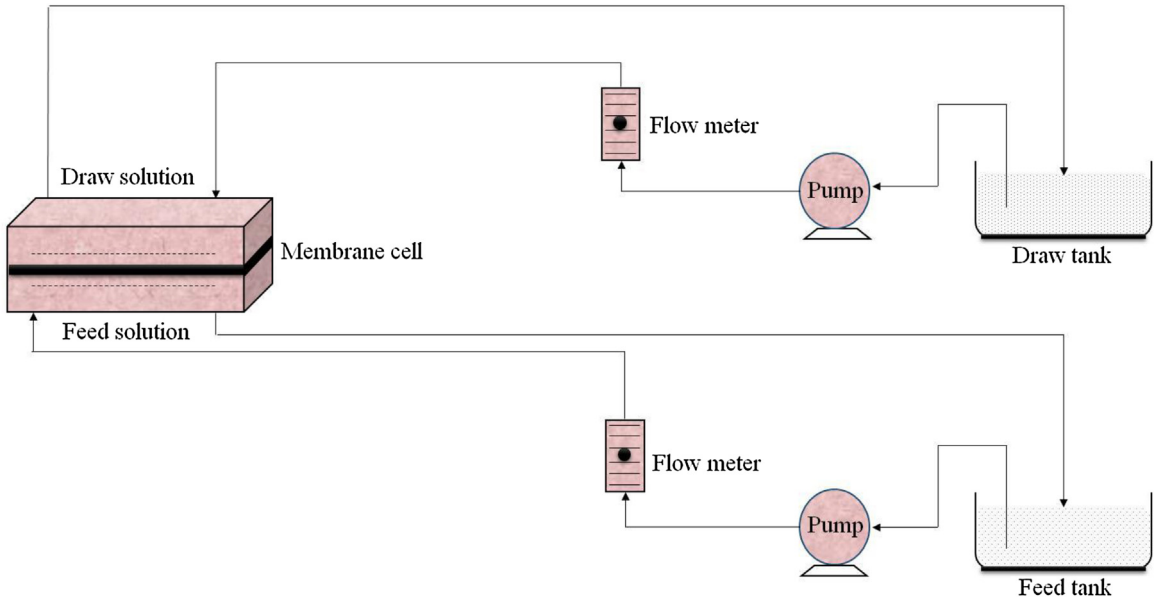


**Fig. 1.** A schematic diagram of the process applied for simulation.

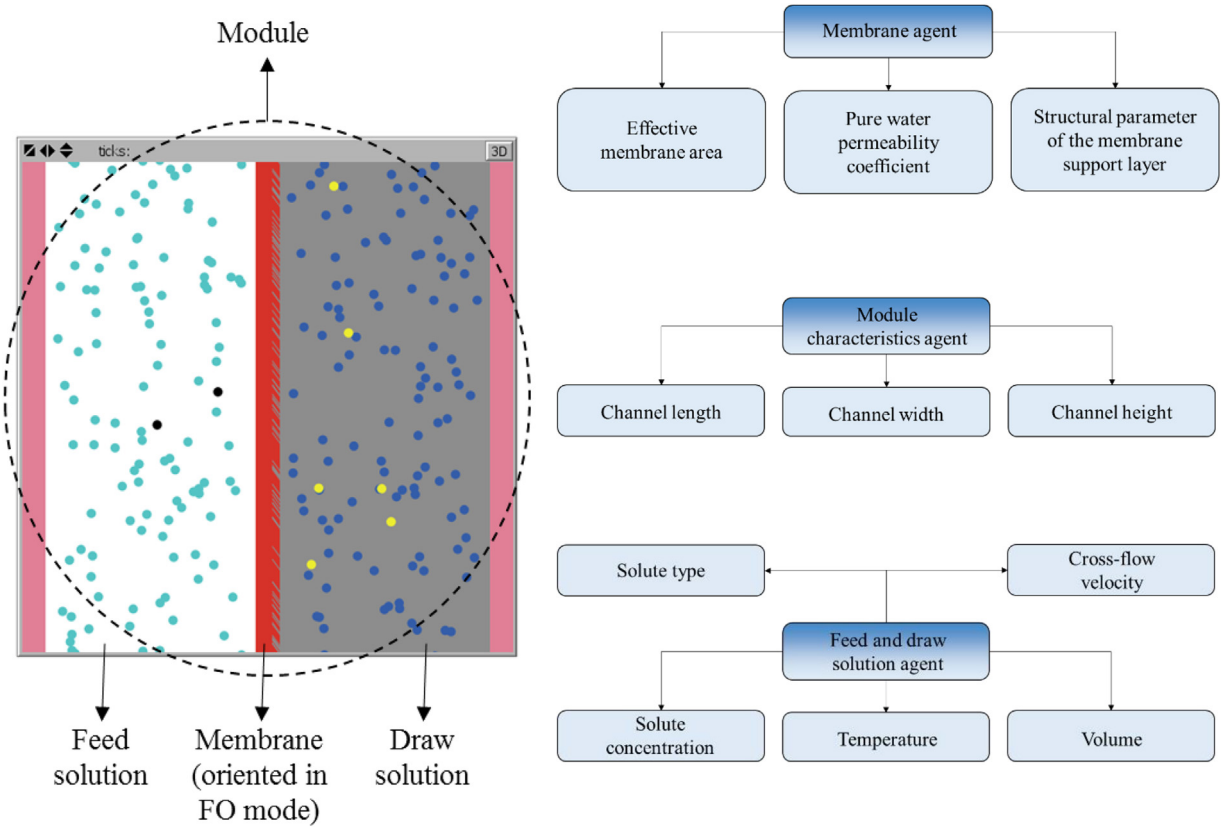


**Fig. 2.** The arrangement of agents in the model's world view and the definition of each agent's specification.

### 2.3. Model development

The forward osmosis simulation model was created using NetLogo 5.0.5 (available at http://ccl.northwestern.edu/netlogo/, developed by Northwestern University Center for Connected Learning and Computer-Based Modeling). Fig. 1 illustrates a schematic diagram of the process used in the system simulation. It was assumed that the proposed model for graphical simulation of FO process composed of two cells, containing an aqueous FS and DS, separated by a semi-permeable membrane (that allows water to pass through and solute to be retained). Thus, three kinds of breed (turtle type) were entirely considered in this model to produce the proposed mechanism, including membrane, module characteristics, and feed and draw solution. The agent-based model including cells and breed (turtle types) is defined in Fig. 2. The membrane agent had specific properties such as effective membrane area,

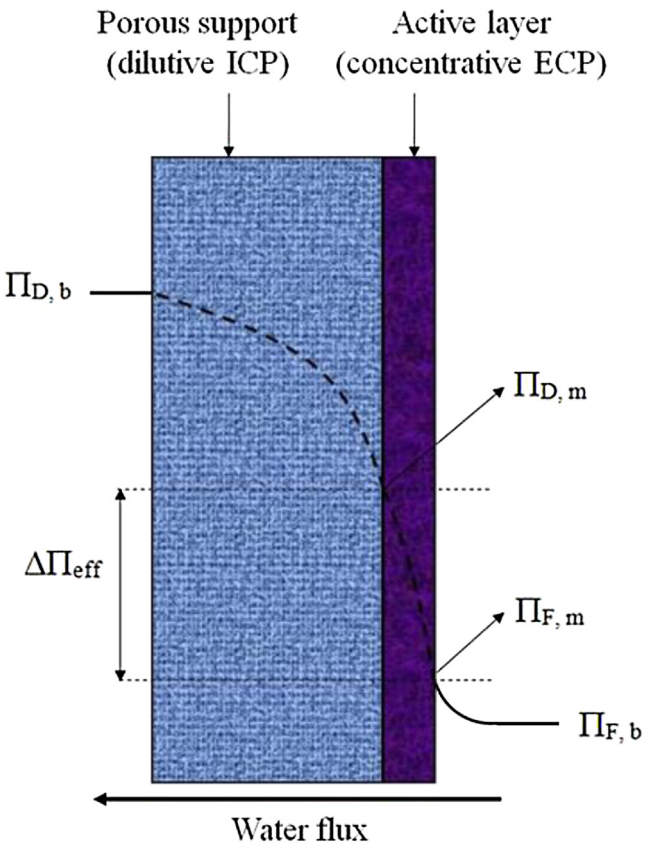


**Fig. 3.** Illustration of concentrative ECP and dilutive ICP in an asymmetric membrane oriented in FO mode.

pure water permeability coefficient, and structural parameter of the membrane support layer specified by users according to their desired membrane characteristics. This breed, shown by red dashed line, separated the model's world into two subspaces. The agent of module characteristics included channel length, width, and height specifications. Moreover, the agent of feed and draw solution had specific features including solute type, solute concentration, temperature, volume, and cross-flow velocity determined by users for each simulation. The solute and water moles of FS and the solute and water moles of DS were seen in the model's platform by black, light blue, yellow, and dark blue circles, respectively. These agents were randomly moved in their cells and also some of water moles crossed the membrane depending on the governing model. The number of these agents was determined by the selected amount of solute concentration and volume of both solutions. A net movement of water moles from the feed side (lower osmotic pressure solution) to the draw compartment (higher osmotic pressure solution) was led to more concentrated FS and more diluted DS progressively until thermodynamic equilibrium was reached (McCutcheon and Elimelech, 2006, 2007). Moreover, the model's environment was comprised of global variables, which were accessible by all agents at any time, such as water flux, osmotic equilibrium, and number of water and solute moles in both solutions.

In many NetLogo models, time passes in discrete steps, called "tick" and tick states the length of a model run. Each tick in the model was assumed to represent one step of separation conducted by the FO process. In each time or tick, solute and water moles of both solutions had a random movement pattern in their cells. In addition, depending on the conditions specified by the user the net movement of water from the FS to the DS side would happen. Thus, as shown in Fig. 3, considering the presence of CP phenomenon at both sides of the membrane in this process, concentrative external CP (ECP) occurs at the membrane surface against the FS and dilutive internal CP (ICP) occurs within the membrane support layer against the DS. This process stopped when the osmotic equilibrium was established between the FS and DS. The osmotic equilibrium concept as the ultimate end of FO process was introduced for the first time by Phuntsho et al. (2014). Another advantage of this model was to consider this concept. At the osmotic equilibrium point, the net transfer of water across the membrane vanished. This balance would occur either at the equal bulk concentrations if the solutes type of both solutions were the same or at the equal bulk osmotic pressures if the solutes type of both solutions were different from each other (Phuntsho et al., 2014).

**Table 1**
Model equations of FO mode.

| Equation | Number |
|---|---|
| $d_h = \frac{2WH}{W+H}$ | (1) |
| $Sc_F = \frac{\mu_F}{\rho_F D_F}$ | (2) |
| $Re_F = \frac{\rho_F v_F d_h}{\mu_F}$ | (3) |
| $Re_F \leq 2100 \rightarrow Sh_F = 1.85(Re_F Sc_F \frac{d_h}{L})^{0.33}$ | (4) |
| $Re_F > 2100 \rightarrow Sh_F = 0.04(Re_F)^{0.75}(Sc_F)^{0.33}$ | (5) |
| $k_F = \frac{Sh_F D_F}{d_h}$ | (6) |
| $K_D = \frac{t\tau}{\varepsilon D_D} = \frac{S}{D_D}$ | (7) |
| $J_{water} = A[\pi_{D,b}\exp(-J_{water}K_D) - \pi_{F,b}\exp(\frac{J_{water}}{k_F})]$ | (8) |
| $n = \frac{(J_{water}\alpha)(\rho_F x_{water,F})}{MW_{water}}\Delta t$ | (9) |
| $m_F = [\frac{(V_{F0}\%V_F)(\rho_F x_{water,F})}{MW_{water}}] - t^*$ | (10) |
| $m_D = [\frac{(V_{D0}\%V_D)(\rho_D x_{water,D})}{MW_{water}}] + t^*$ | (11) |
| $V_{F,new} = V_{F0} - [\frac{t^* MW_{water}}{\rho_F x_{water,F}}]$ | (12) |
| $V_{D,new} = V_{D0} + [\frac{t^* MW_{water}}{\rho_D x_{water,D}}]$ | (13) |
| $C_{F,new} = \frac{C_{F0}V_{F0}}{V_{F,new}}$ | (14) |
| $C_{D,new} = \frac{C_{D0}V_{D0}}{V_{D,new}}$ | (15) |

For agent-based simulation approach, an algorithm was developed according to the reliable and suitable models for FO mode (dilutive ICP and concentrative ECP), which were previously applied successfully by other researches (McCutcheon and Elimelech, 2006, 2007; Phuntsho et al., 2012). Furthermore, this code was written to be used in agent-based model.

Clearly, any modeling study contains suitable and reasonable assumptions. Accordingly, in the current study, the FO model incorporated ECP and ICP phenomena. In addition, the model was developed using the following assumptions:

- The membrane characteristics were considered uniform.
- Temperature variation was neglected during the process time.
- The ECP effect was defined according to the boundary layer film theory.
- The ratio of solute concentration was considered approximately proportional to that of the osmotic pressure.
- The membrane fully rejected the solute and the solute permeability was negligible.

The iteration procedures and related equations used to solve the FO mode are reported in Fig. 4 and Table 1, respectively. It should be noted that some of the equations presented in Table 1 were obtained from the literature (McCutcheon and Elimelech, 2006, 2007; Phuntsho et al., 2012).

After running the simulation of FO process, output data were exported into Microsoft Excel spreadsheets and finally statistical parameters (for model validation) were calculated using the model and experimental data.

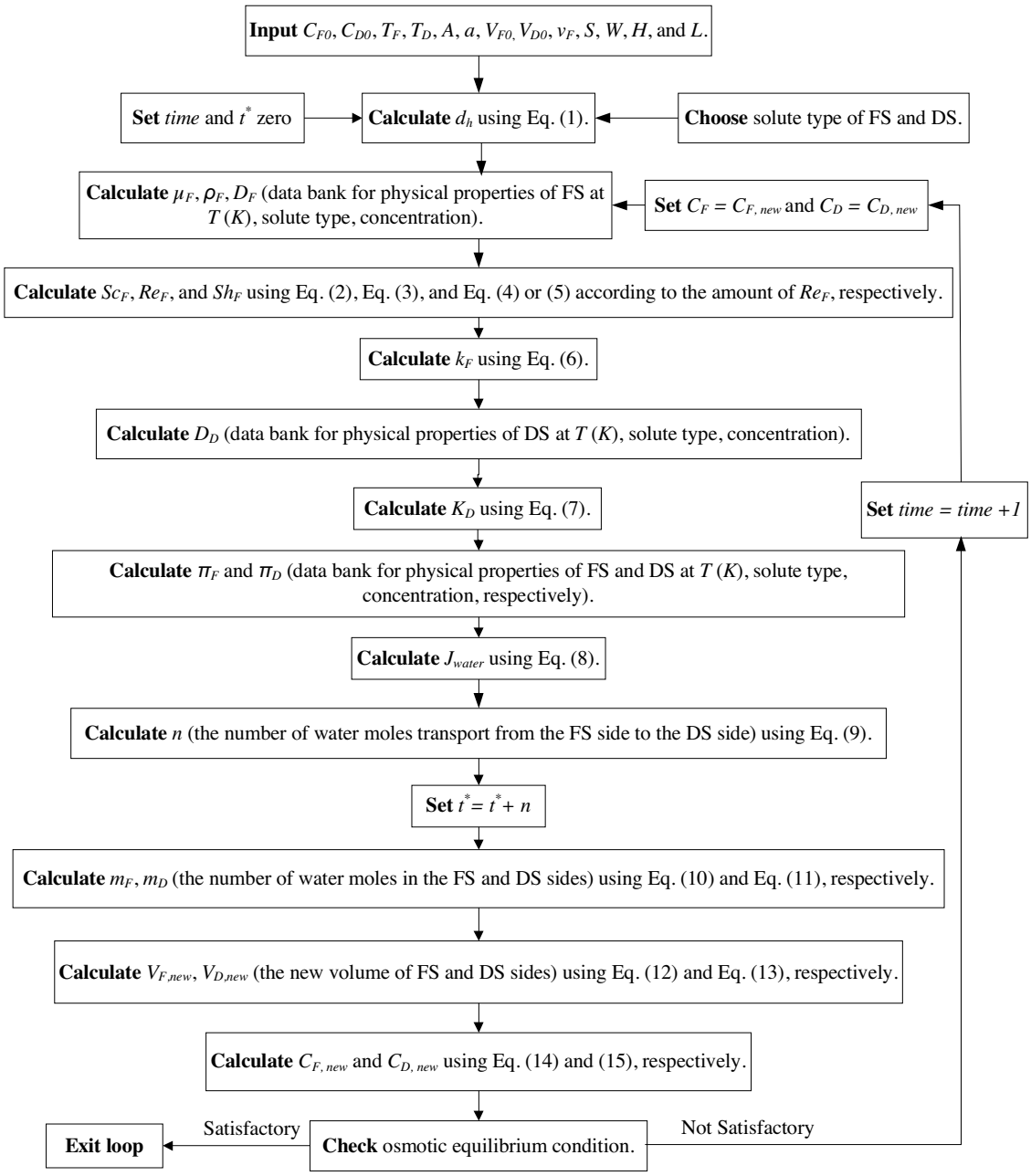


**Fig. 4.** Iteration algorithm for solving the FO mode model.

## 3. Results and discussion

### 3.1. Building the model

Fig. 5 illustrates the developed model interface in the Netlogo platform. As can be seen in Fig. 5(a), it was required to set the input parameters by the user from the graphical user interface including solute concentration, temperature, cross-flow velocity, volume and solute type of FS and DS, channel dimensions of cell, pure water permeability coefficient of membrane, structural parameter of membrane support layer, and effective membrane area.

Fig. 5(b) also shows the output parameters of FO mode model in the NetLogo platform. The principal output of this NetLogo platform was the plot of average water flux. In addition, the plots of volume, density, dynamic viscosity, solute diffusion coefficient, osmotic pressure, Reynolds number, Schmidt number, Sherwood number, solute resistivity for diffusion within the porous support layer, and mass transfer coefficient of FS and DS were reported in the graphical user interface. As can be observed in this Figure, there are also some monitors for displaying instantaneous value of mentioned plots and osmotic equilibrium time. It should be noted that one advantage of this model was to consider the changes which may happen in process parameters as long as the simulation is running. Consequently, it led to the improvement of the simulator outputs and approaching to the real conditions.

The simulation parameters are described in details in Table 2. It is also important to note that the proposed model extensively incorporated the data library to determine various solution properties. These properties were collected from different trustworthy references. Some of them are reported in Appendix A.

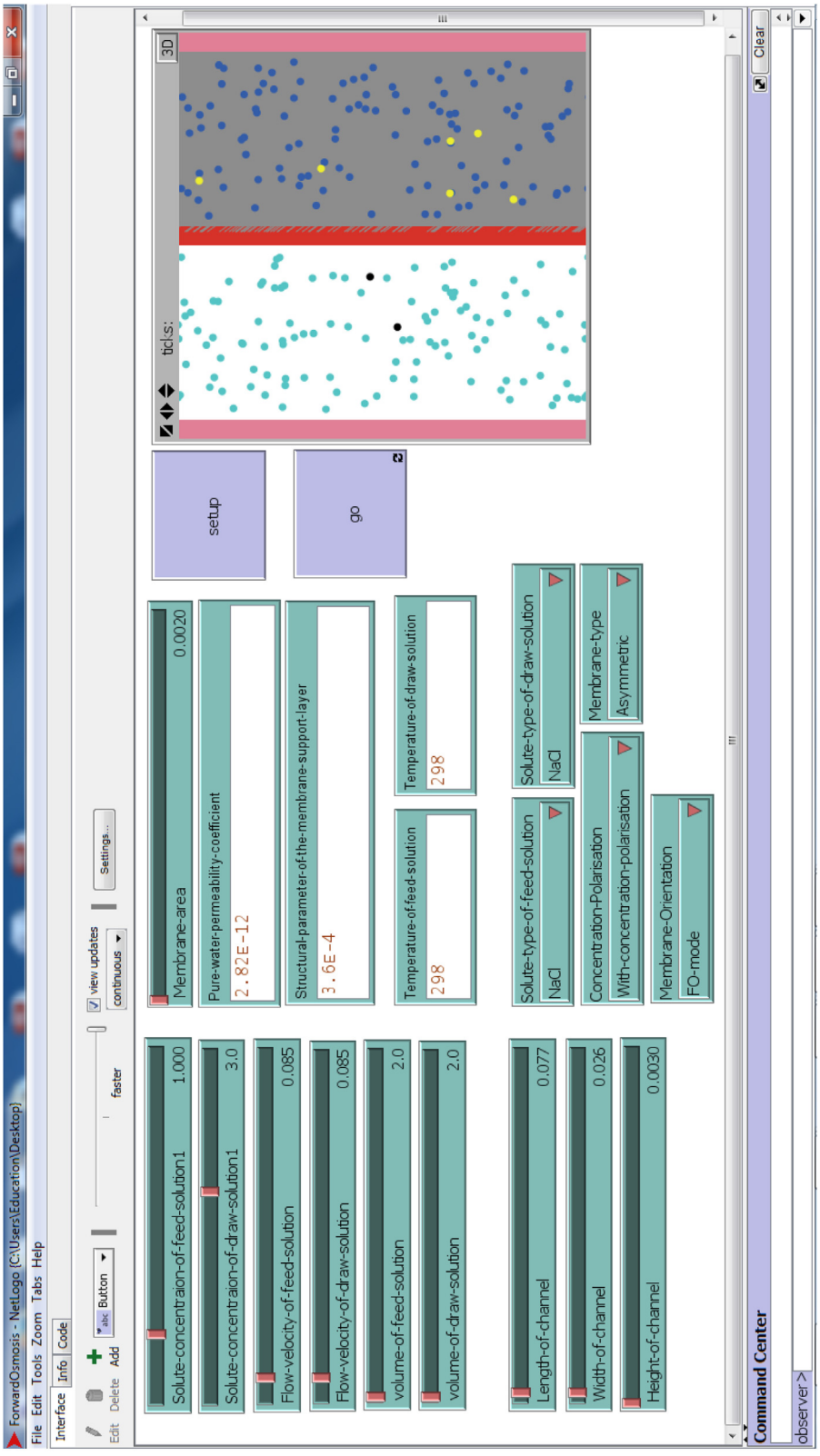


(a)

**Fig. 5.** The developed model interface in the Netlogo platform (a) input parameters and (b) output parameters.

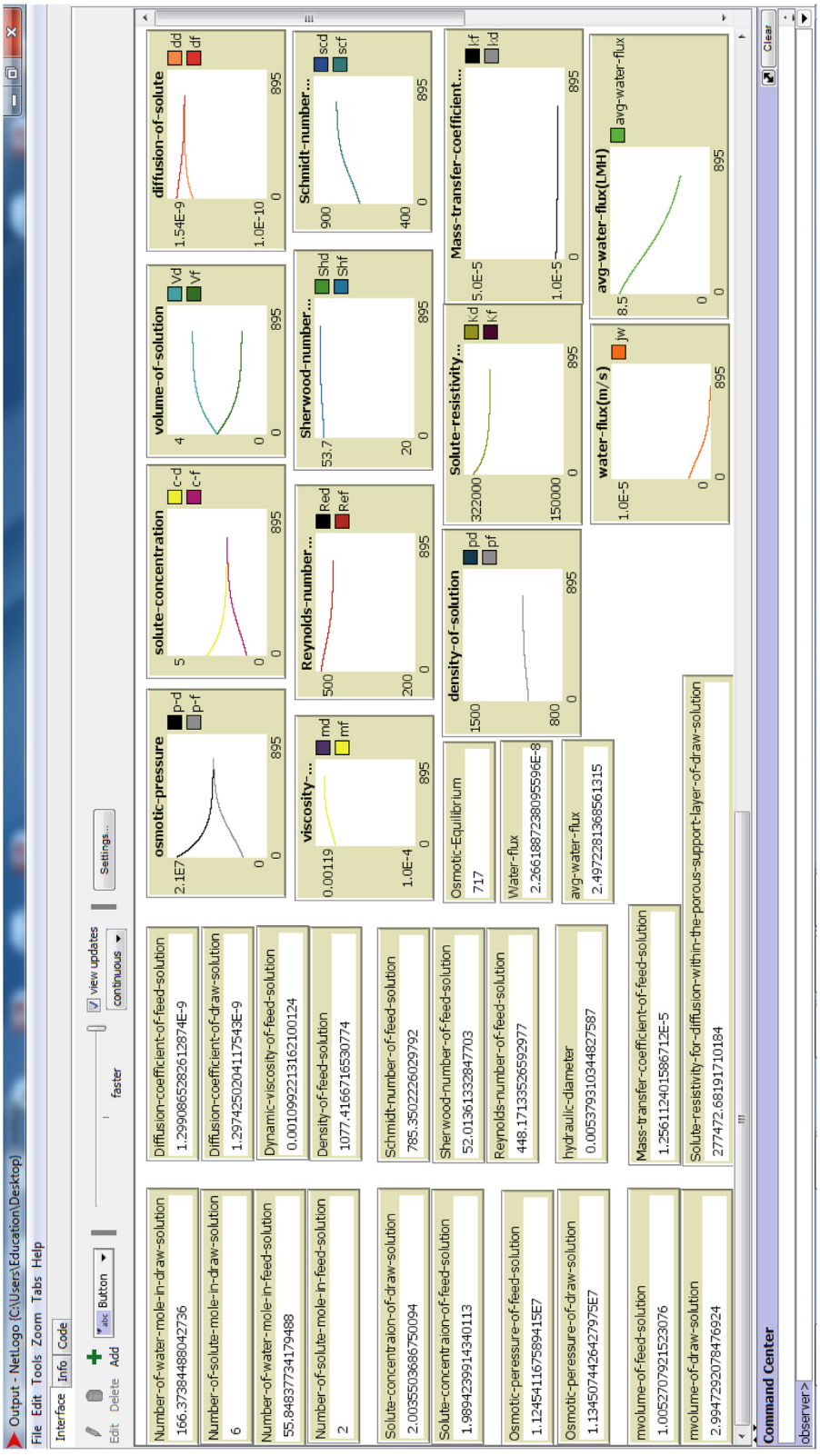


(b)

**Fig. 5.** (*Continued*)

**Table 2**
Simulation parameters (baseline data) (Phuntsho et al., 2012).

| Model parameter | Value |
|---|---|
| Solute type of FS | NaCl |
| Solute type of DS | NaCl |
| Concentration polarization | With CP consideration |
| Membrane type | Asymmetric |
| Membrane orientation | FO mode |
| Volume of FS ($V_F$, l) | 2 |
| Volume of DS ($V_D$, l) | 2 |
| Solute concentration of FS ($C_F$, mol/l) | 0 (DI water) 2 |
| Solute concentration of DS ($C_D$, mol/l) | 3 |
| Temperature of FS ($T_F$, K) | 298 |
| Temperature of DS ($T_D$, K) | 298 |
| Channel length ($L$, m) | 0.077 |
| Channel width ($W$, m) | 0.026 |
| Channel height ($H$, m) | 0.003 |
| Cross-flow velocity of FS ($v_F$, m/s) | 0.085 |
| Cross-flow velocity of DS ($v_D$, m/s) | 0.085 |
| Pure water permeability coefficient ($A$, m/Pa s) | 2.82E-12 |
| Structural parameter of the membrane support layer ($S$, m) | 3.6E-4 |
| Membrane area ($a$, $m^2$) | 0.002 |

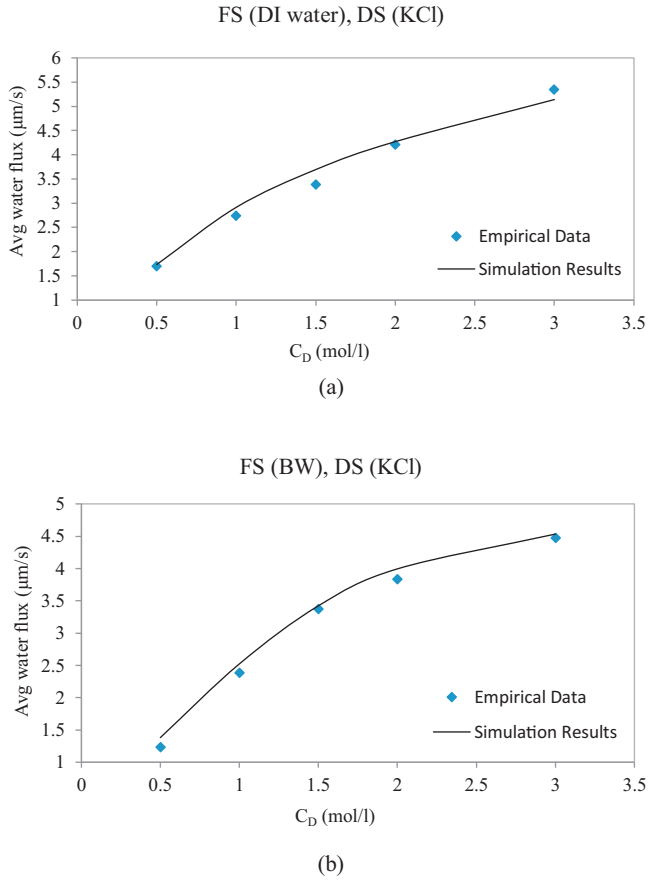


**Fig. 6.** Comparison of experimental water flux results from Phuntsho et al. (2012) and the modeling outputs in the case using (a) DI water and (b) BW as FSs.

**Table 3**
Percentage of standard deviation and error.

| Feed solution | % Error | % SD |
|---|---|---|
| DI water BW | 4.3963 4.5604 | 6.0495 7.0365 |

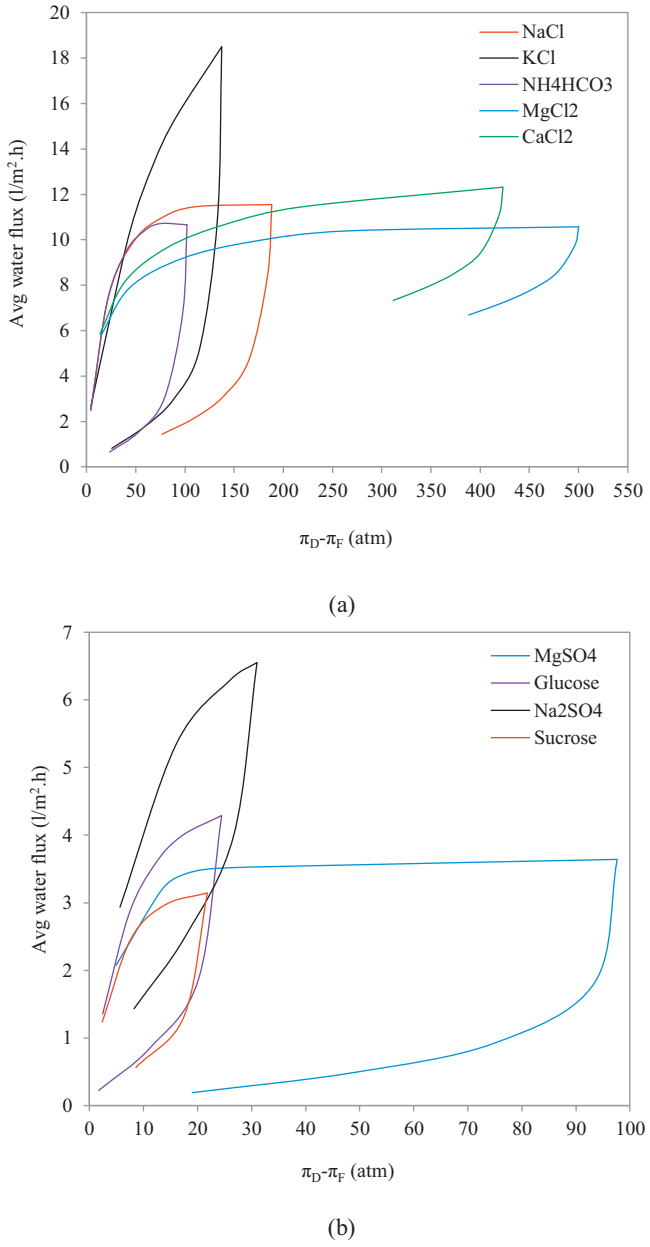


**Fig. 7.** Effect of net bulk osmotic pressure on average water flux for (a) NaCl, KCl, $NH_4HCO_3$, $MgCl_2$, $CaCl_2$ and (b) $MgSO_4$, Glucose, $Na_2SO_4$, Sucrose.

### 3.2. Model validation

The precision and reliability of this model were established by its ability to provide an environment for simulation of a real FO process. Therefore, validation of the model was an important and necessary step in the simulation. For this purpose, experimental water flux data reported by Phuntsho et al. (2012) for dilution of 0.5–3.0 Molar aqueous KCl solutions by FO was used as a case study to validate the simulation model based upon NetLogo environment. A cellulose triacetate (CTA) FO membrane (the characteristics of this membrane have been widely presented (Cath et al., 2006; McCutcheon et al., 2005; Tang et al., 2010)) was the permeable barrier for separation of DI water or BW as FS and KCl in pure water as DS. The bench-scale cross-flow FO unit was made up of symmetric cells on both sides of the membrane with dimensions of 0.026 m width, 0.077 m length, and 0.003 m depth. The cross-flow was in a counter-current mode at 0.085 m/s. More information on

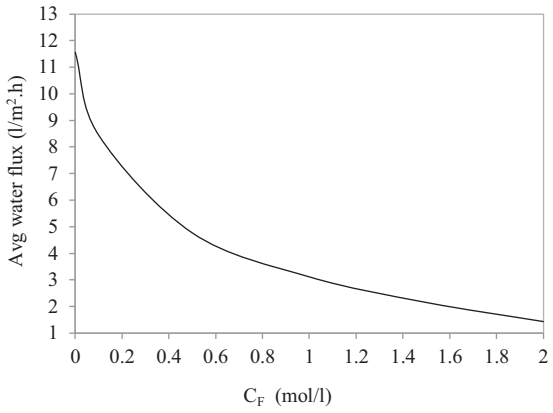


**Fig. 8.** Average water flux versus various concentrations of FS according to the simulation parameters (baseline data).

the experimental system and conditions can be found in the literature (Phuntsho et al., 2012). The simulation model platform was run by using the operational conditions of Phuntsho et al. study to investigate the water flux profile. It is important to mention that the standard deviation and error percentage of the data were estimated using two following equations (Abramowitz and Stegun, 1964; Juang et al., 2010):

$$\%SD = 100 \times \sqrt{\left( \sum_{n} \frac{\left[1 - \left(C_{\mathrm{mod}\,el}/C_{emp}\right)\right]^2}{n-1} \right)} \tag{16}$$

$$\%Error = 100 \times \left( \frac{1}{n} \sum_{n} \left| \frac{C_{\mathrm{mod}\,el} - C_{emp}}{C_{\mathrm{mod}\,el}} \right| \right) \tag{17}$$

where $n$ is the number of data, $C_{model}$ is the modeling results, and $C_{emp}$ is the empirical data.

According to Fig. 6, trend of changes in water flux was well predicted by the agent-based model simulation. The model errors are presented in Table 3. The results have shown a good agreement between outputs obtained from the simulation and empirical data in the case using both DI water and BW as FS. As a result, the agent-based model provided a good simulation of FO mode.

### 3.3. Effect of net bulk osmotic pressure

In order to investigate the influence of bulk osmotic pressure difference between the DS and FS, the following simulation protocol was used for various draw solutes. The simulator platform was first run by using DI water as FS and incrementally increasing the DS concentration up to the specified concentration (depending on the available data for each solute and considering the assumption mentioned in Section 2.3 for the ratio of solute concentration which is reasonable for relatively dilute solutions), to examine the ICP effect.

After the flux determination was taken at the final DS concentration with DI water feed, a subsequent increase in NaCl FS concentration was applied while keeping the specified concentration of DS constant, to investigate simultaneously the ICP and ECP effects.

For this purpose, nine different solutes which are the most widely used as solute of DS in FO process were selected. It is necessary to mention that there are some features for selecting a DS such as being highly soluble and recoverable, economical possibility, and being easily separable from water (Cath et al., 2006; Jung et al., 2011). Fig. 7 shows the effect of net bulk osmotic pressure known as the driving force of FO process versus average water flux for various DSs. According to the aforementioned simulation protocol, the logarithmic increase in average water flux with an increase in effective osmotic pressure difference can be seen in the ascending line of each solute. It was completely attributed to the dilutive ICP because the feed was DI water. When the concentration of NaCl as FS was raised, the flux suddenly declined due to the combined effect of dropped osmotic pressure difference and concentrative ECP. It should be also taken into account that each draw solute, with respect to the driving force that creates, can produce different amounts of water flux. Similar flux behaviors were observed in the previous studies (McCutcheon and Elimelech, 2006; McCutcheon et al., 2005, 2006).

### 3.4. Effect of the different parameters on water flux

According to the proposed model and simulation parameters, the variation of average water flux with respect to the different concentrations of FS is shown in Fig. 8. The FO was simulated under the conditions presented in Table 2 while maintaining the concentra-

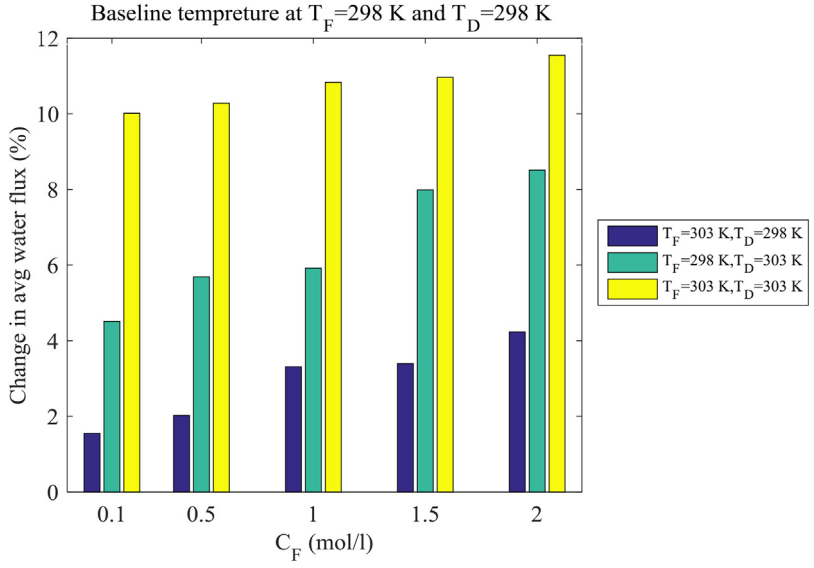


**Fig. 9.** Effect of FS and DS temperature on percentage of changes in average water flux.

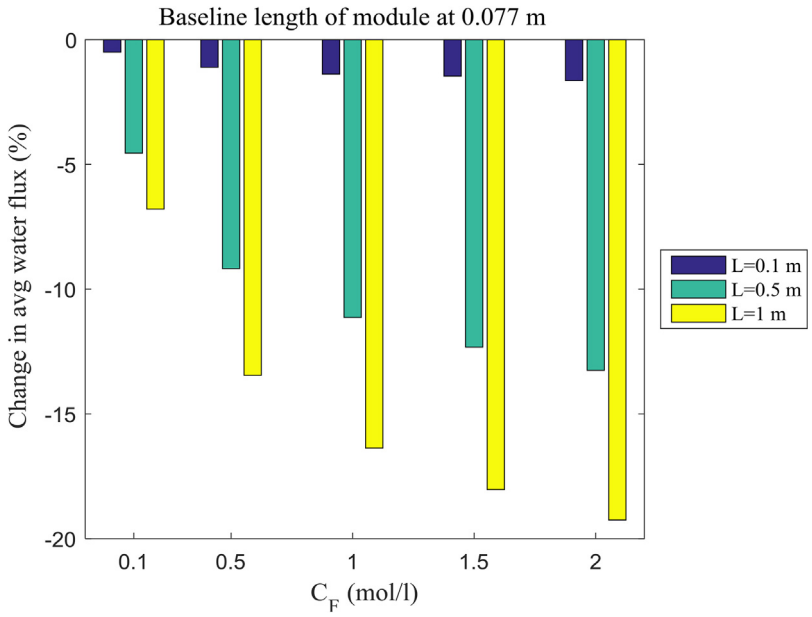


**Fig. 10.** Effect of length of module on percentage of changes in average water flux.

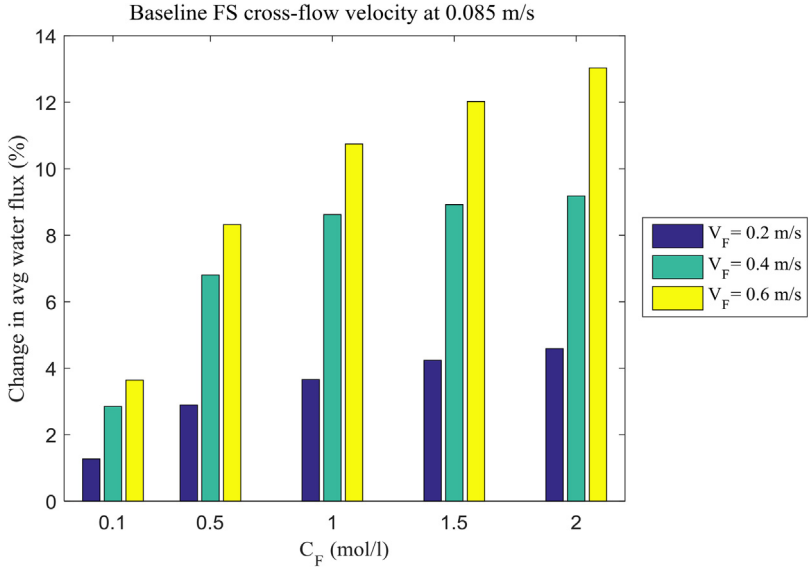


**Fig. 11.** Effect of FS cross-flow velocity on percentage of changes in average water flux.

tion of DS at 3.0 Molar and changing the concentration of FS from 0 to 2.0 Molar. The influence of some parameters, in the following sections, including temperature, length of module, cross-flow velocity, pure water permeability coefficient, and structural parameter of membrane were compared to this base condition.

### 3.4.1. *Effect of temperature*

The influence of temperature on percentage of changes in average water flux was investigated in three different states of FS and DS temperature compared to the base condition. As shown in Fig. 9, temperature has a positive effect on water flux. Generally, temperature can affect the osmotic pressure and thermodynamic properties of solutions such as viscosity and diffusion coefficient (McCutcheon and Elimelech, 2006; Phuntsho et al., 2012). Based upon monitoring of simulation parameters in the platform, by increasing the temperature of each solution, dynamic viscosity was decreased but diffusion coefficient of solutes and osmotic pressure were raised.

On the one hand, when the temperature of FS was increased, the net osmotic pressure for driving the water in FO process was reduced. However, increasing the mass transfer coefficient of FS ($k_F$), due to the rise of diffusion coefficient, resulted in reducing the ECP modulus (McCutcheon and Elimelech, 2006). On the other hand, the growth in temperature of DS led to the increase in the net driving force of FO process. Furthermore, the increase in diffusion coefficient was expected to ultimately lower the solute resistivity of membrane support layer as indicated by Eq. (7), subsequently declining the ICP effects. These results confirm those of other researches which investigated the effects of temperature on water flux (McCutcheon and Elimelech, 2006; Phuntsho et al., 2012).

### 3.4.2. *Effect of length of module*

Fig. 10 displays the effect of length of module on percentage of changes in average water flux of the FO process in three various conditions of length compared to the base condition. The increase

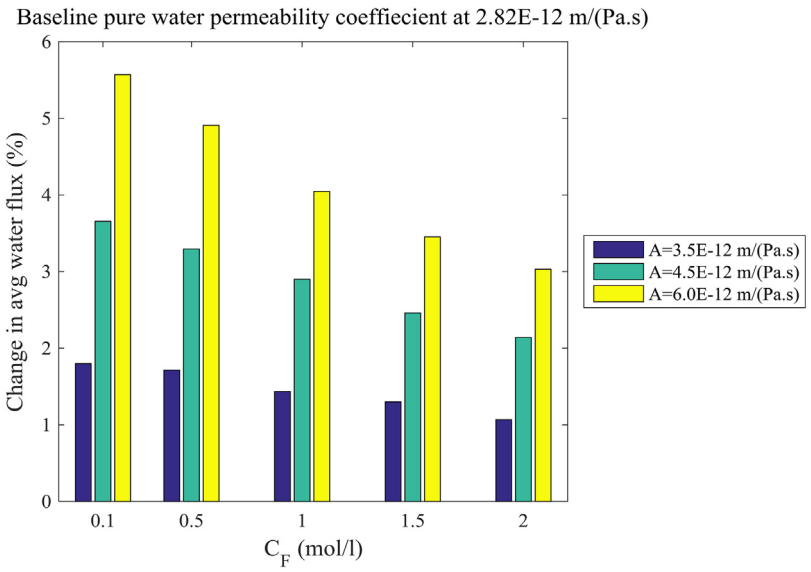


**Fig. 12.** Effect of pure water permeability coefficient on percentage of changes in average water flux.

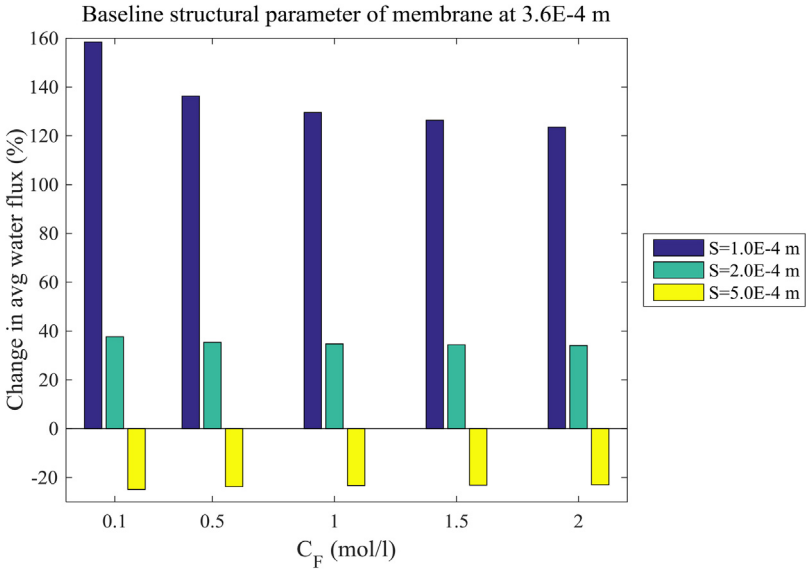


**Fig. 13.** Effect of structural parameter of membrane on percentage of changes in average water flux.

in the length of module resulted in the decrease of water flux. It was due to the decreased concentration difference of FS and DS, thereby reducing the net driving force of FO, as the length of module increases (Shim and Kim, 2013). Moreover, it is important to mention that the effect of ECP modulus as an undesirable impact was more severe by increasing the solute concentration of FS.

### 3.4.3. *Effect of FS cross-flow velocity*

The effect of FS cross-flow velocity on percentage of changes in average water flux was studied in three different values of FS cross-flow velocity compared to the base condition. It can be observed in Fig. 11 that increasing the cross-flow velocity of FS increased the percentage of average water flux. This was generally attributed to the rise of mass transfer coefficient of FS ($k_F$) which led to the decline of ECP modulus and enhancement of water flux (Jung et al., 2011). Thus, negative effects of ECP can be reduced by increasing cross-flow velocity and turbulence. However, the adverse influence of ICP cannot be decreased by changing the cross-flow velocity because it occurs within the porous support layer (Cath et al., 2006).

### 3.4.4. *Effect of pure water permeability coefficient*

The influence of various values of pure water permeability coefficient on percentage of changes in average water flux compared to the base condition is presented in Fig. 12. As indicated by Eq. (8), pure water permeability coefficient has a direct effect on the obtained water flux. As pure water permeability coefficient was increased, the average water flux was raised. However, by increasing the concentration of FS, due to the rise in adverse influence of ECP, the percentage gain in average water flux was gradually decreased. Therefore, enhancement in membrane characteristics by increasing water permeability is an approach to improve water flux (Jung et al., 2011).

### 3.4.5. *Effect of structural parameter of membrane*

The structural parameter of membrane includes thickness ($t$), tortuosity ($\tau$), and porosity ($\varepsilon$). This parameter indicates the extent of ICP within the porous support layer. As the membrane thickness and tortuosity decrease (considering that control of tortuosity is more difficult) and the membrane porous support layer becomes

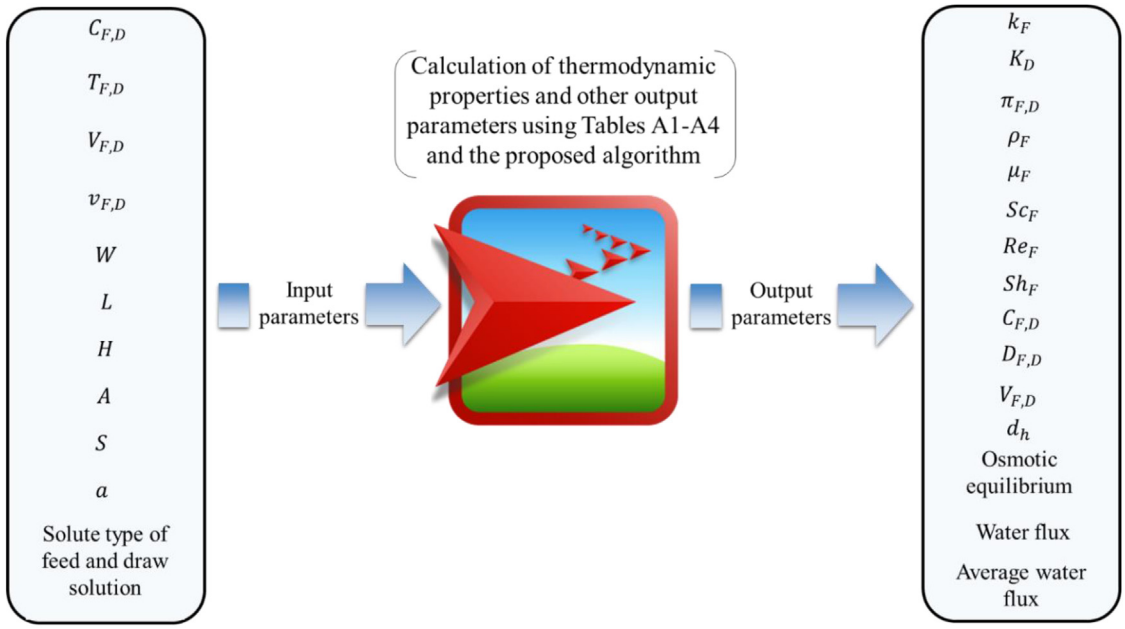


(a)

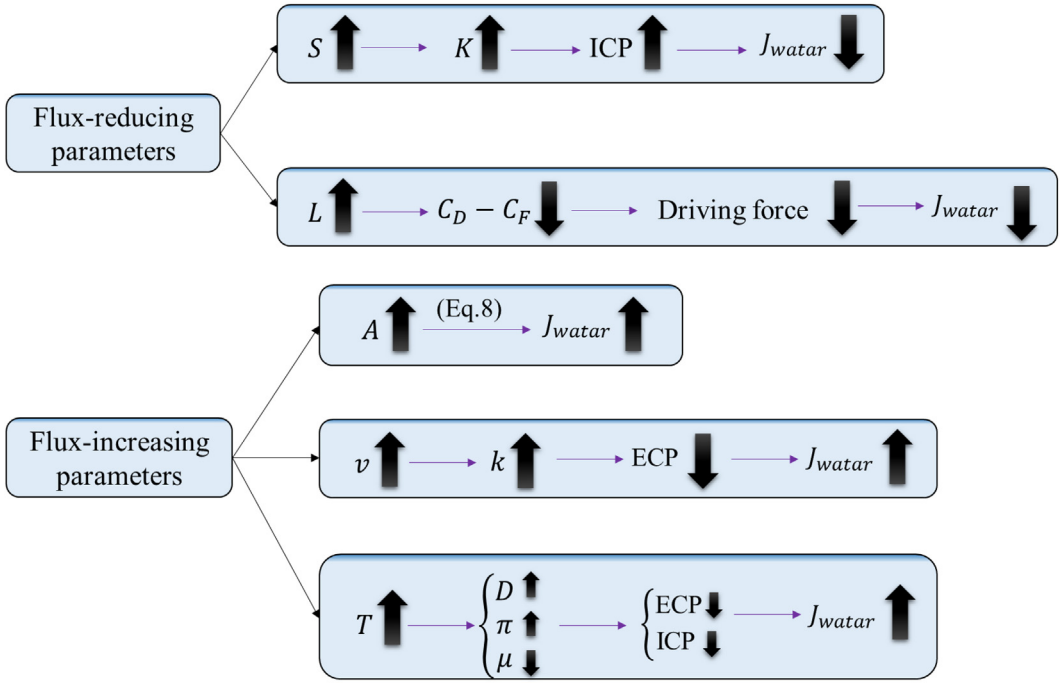


(b)

**Fig. 14.** A schematic diagram of (a) the overall relationship between input and output parameters and (b) the effects of process parameters on the water flux.

more porous, as shown in Eq. (7), the ICP effect can be reduced (Dabaghian and Rahimpour, 2015; McCutcheon and Elimelech, 2006). From the results shown in Fig. 13, as the structural parameter of membrane increased, the water flux was reduced due to the rise of solute resistivity. In addition, by increasing the amount of FS concentration, owing to the combined adverse influence of ECP and ICP, the percentage of average water flux was declined. These findings are in agreement with other previous researches results (Jung et al., 2011; McCutcheon and Elimelech, 2006).

### 3.5. Overall relationship between input and output parameters

The influence of some process parameters have been discussed above. Fig. 14 illustrates the overall relationship between input and output parameters. As can be seen in Fig. 14(a), after entering the input parameters, calculating the thermodynamic parameters using Tables A1–A4, and employing the presented algorithms, output parameters are determined. Furthermore, Fig. 14(b)

schematically represents the effects of process parameters on the water flux.

## 4. Conclusions

In this study, an agent-based model for simulation of FO mode was developed for the first time using the NetLogo platform. Furthermore, the dynamic of FO process was represented in order to comprehend its complex behavior. This simulation model allows researchers to have a better prediction and understanding of the output of FO process. Some of the advantages of the proposed model were as follows: being accessible for even non-expert users, providing the facility and flexibility for predicting the FO process performance at various scenarios, investigating the potential of different solutes as DS, and developing visualization tools in the graphical user interface to show the dynamic of process.

The influence of process parameters, including temperature, length of module, FS cross-flow velocity, pure water permeability coefficient, and structural parameter of membrane on average water flux was studied. The simulation outputs revealed that among the different process parameters, increase in length of module and structural parameter of membrane had negative impact on average water flux. The experimental water flux data obtained from applying FO mode by commercial CTA membrane for diluting KCl solution with DI water and BW solutions were also successfully used as case study to validate the NetLogo platform.

This Simulation model provided the ability to test wide variety of scenarios in a very short time (due to the model flexibility and facility for creating different scenarios rapidly) and without actually conducting a physical experiment in order to achieve the optimal conditions.

## Appendix A. Solution and solute properties

The coefficients used in each of the polynomial equations for various physical properties of solutions are tabulated in Tables A1–A4.

**Table A1**
Coefficients of polynomial equations used for determination of dynamic viscosity of solutions.

| Dynamic viscosity ($\mu[Pa.s]$, $C$ $[Molar]$) $\mu = \alpha + \beta C + \gamma C^2 + \delta C^3 + \theta C^4$ | | | | | | | |
|---|---|---|---|---|---|---|---|
| Solute | Coefficient($\times 10^{-6}$) | | | | | Remarks | Ref. |
| | $\alpha$ | $\beta$ | $\gamma$ | $\delta$ | $\theta$ | | |
| NaCl | 890.7 | 70 | 1.75 | – | – | @298 $K$ | (Sagiv et al., 2014) |
| NaCl | 798.1 | 64 | 16 | – | – | @303 $K$ | (Sagiv et al., 2014) |
| KCl | 846 | 3.5 | – | – | – | @298 $K$ | (Sagiv et al., 2014) |
| $NH_4HCO_3$ | 897.1 | 320 | −4.5 | – | – | @298 $K$ | (Sagiv et al., 2014) |
| $NH_4HCO_3$ | 798.1 | 291 | −7 | – | – | @303 $K$ | (Sagiv et al., 2014) |
| $Na_2SO_4$ | 890 | 428.5 | – | – | – | @298 $K$ For $C \leq 0.65$ $Molar$ | (Geraldes et al., 2001) |
| Sucrose | 890 | 375 | 1550.1 | – | – | @298 $K$ For $C \leq 1.1$ $Molar$ | (Geraldes et al., 2001) |
| $MgSO_4$ | 889 | 647 | −505 | 215 | – | @298 $K$ | (Laliberté, 2007) |
| $MgCl_2$ | 882 | 397 | −71 | 70.9 | – | @298 $K$ | (Laliberté, 2007) |
| $CaCl_2$ | 904 | −45.9 | 467 | −178 | 28.1 | @298 $K$ | (Laliberté, 2007) |
| Glucose | $\mu = 2.0041 \times 10^{-6} \times \exp(-0.4324C) \times \exp(\frac{242.58C+1889.3}{298})$ | | | | | @298 $K$ | (Bui and Nguyen, 2004) |

**Table A2**
Coefficients of polynomial equations used for determination of density of solutions.

| Density ($\rho[kg/m^3]$, $C$ $[Molar]$) $\rho = \alpha + \beta C + \gamma C^2 + \delta C^3$ | | | | | | |
|---|---|---|---|---|---|---|
| Solute | Coefficient | | | | Remarks | Ref. |
| | $\alpha$ | $\beta$ | $\gamma$ | $\delta$ | | |
| NaCl | 996.845 | 40.5 | – | – | @298 $K$ | (Sagiv et al., 2014) |
| NaCl | 995.404 | 40 | – | – | @303 $K$ | (Sagiv et al., 2014) |
| KCl | 997.048 | 48 | 1.04 | – | @298 $K$ | (Sagiv et al., 2014) |
| $NH_4HCO_3$ | 996.84 | 31 | −1.2 | – | @298 $K$ | (Sagiv et al., 2014) |
| $NH_4HCO_3$ | 995.404 | 30.5 | −1.18 | – | @303 $K$ | (Sagiv et al., 2014) |
| $Na_2SO_4$ | 997.1 | 124.332 | – | – | @298 $K$ For $C \leq 0.65$ $Molar$ | (Geraldes et al., 2001) |
| Sucrose | 997.1 | 134.058 | – | – | @298 $K$ For $C \leq 1.1$ $Molar$ | (Geraldes et al., 2001) |
| $MgSO_4$ | 997 | 109 | – | – | @298 $K$ | (Laliberté, 2007) |
| $MgCl_2$ | 1000 | 69.2 | – | – | @298 $K$ | (Laliberté, 2007) |
| $CaCl_2$ | 1000 | 78.3 | – | – | @298 $K$ | ("OLI Stream Analyser 3.2") |
| Glucose | 1000 | 55.4 | −4.05 | 0.118 | @298 $K$ | (Castaldi et al., 1998) |

**Table A3**
Coefficients of polynomial equations used for determination of diffusivity of solutions.

| Diffusivity ($D[m^2/s]$, $C$ $[Molar]$) $D = \alpha + \beta C + \gamma C^2 + \delta C^3 + \theta C^4$ | | | | | | | |
|---|---|---|---|---|---|---|---|
| Solute | Coefficient($\times 10^{-12}$) | | | | | Remarks | Ref. |
| | $\alpha$ | $\beta$ | $\gamma$ | $\delta$ | $\theta$ | | |
| NaCl | 1570 | −360 | 300 | – | – | @298 $K$ For $C < 0.528$ $Molar$ | (Sagiv et al., 2014) |
| NaCl | 1509 | −94 | −6 | – | – | @298 $K$ For $0.528 \leq C < 3.5$ $Molar$ | (Sagiv et al., 2014) |
| NaCl | 1780 | −700 | 1500 | −1200 | – | @303 $K$ For $C < 0.315$ $Molar$ | (Sagiv et al., 2014) |
| NaCl | 1707 | −116 | −4 | – | – | @303 $K$ For $0.315 \leq C < 3.5$ $Molar$ | (Sagiv et al., 2014) |

Table A3 (*Continued*)

| Diffusivity ($D$[$m^2/s$], $C$ [*Molar*]) $D = \alpha + \beta C + \gamma C^2 + \delta C^3 + \theta C^4$ | | | | | | | |
|---|---|---|---|---|---|---|---|
| Solute | Coefficient($\times 10^{-12}$) | | | | | Remarks | Ref. |
| | $\alpha$ | $\beta$ | $\gamma$ | $\delta$ | $\theta$ | | |
| KCl | 1880 | 90 | 14 | – | – | @298 *K* | (Sagiv et al., 2014) |
| $NH_4HCO_3$ | 1429 | −66 | 186 | – | – | @298 *K* For $C < 0.481$ *Molar* | (Sagiv et al., 2014) |
| $NH_4HCO_3$ | 1390 | 96 | 10 | – | – | @298 *K* For $0.481 \leq C < 3.11$ *Molar* | (Sagiv et al., 2014) |
| $NH_4HCO_3$ | 1608 | −82 | 231 | – | – | @303 *K* For $C < 0.425$ *Molar* | (Sagiv et al., 2014) |
| $NH_4HCO_3$ | 1560 | 102 | 95 | – | – | @303 *K* For $0.425 \leq C < 3.12$ *Molar* | (Sagiv et al., 2014) |
| $Na_2SO_4$ | $D = 1.23 \times 10^{-9} - 4.22 \times 10^{-10} C^{0.4}$ | | | | | @298 *K* For $C \leq 0.65$ *Molar* | (Geraldes et al., 2001) |
| Sucrose | 0.52 | −0.222 | – | – | – | @298 *K* For $C \leq 1.1$ *Molar* | (Geraldes et al., 2001) |
| $MgSO_4$ | 601 | −425 | 303 | −107 | 14 | @298 *K* | (Rard and Miller, 1979a) |
| $MgCl_2$ | 1030 | 38 | 64 | −38 | 4 | @298 *K* | (Miller et al., 1984) |
| $CaCl_2$ | 1110 | 43 | 96 | −41 | 3 | @298 *K* | (Rard and Miller, 1979b) |
| Glucose | 666 | −143 | 16 | −0.7 | – | @298 *K* | (Castaldi et al., 1998) |

**Table A4**
Coefficients of polynomial equations used for determination of osmotic pressure of solutions.

| Osmotic pressure ($\pi$[Pa], $C$ [Molar]) $\pi = \alpha + \beta C + \gamma C^2 + \delta C^3 + \theta C^4 + \phi C^5 + \sigma C^6$ | | | | | | | | | |
|---|---|---|---|---|---|---|---|---|---|
| Solute | Coefficient($\times 10^5$) | | | | | | | Remarks | Ref. |
| | $\alpha$ | $\beta$ | $\gamma$ | $\delta$ | $\theta$ | $\phi$ | $\sigma$ | | |
| NaCl | – | 42.6 | 7 | – | – | – | – | @298 K | (Sagiv et al., 2014) |
| NaCl | – | 42.8 | 7.1 | – | – | – | – | @303 K | (Sagiv et al., 2014) |
| KCl | – | 45 | 0.47 | – | – | – | – | @298 K | (Sagiv et al., 2014) |
| $NH_4HCO_3$ | – | 44.1 | −3.2 | – | – | – | – | @298 K | (Sagiv et al., 2014) |
| $NH_4HCO_3$ | – | 45 | −3.2 | – | – | – | – | @303 K | (Sagiv et al., 2014) |
| $Na_2SO_4$ | $\pi = 51.0082 \times 10^5 C^{0.95}$ | | | | | | | @298 K For $C \leq 0.65$ *Molar* | (Geraldes et al., 2001) |
| Sucrose | – | 23.22 | 7.02 | 7.04 | – | – | – | @298 K For $C \leq 1.1$ *Molar* | (Geraldes et al., 2001) |
| $MgSO_4$ | −1.19 | 73.8 | −130.44 | 95.32 | −26.81 | 2.93 | −0.08 | @298 K | ("OLI Stream Analyser 3.2") |
| $MgCl_2$ | 9.16 | 51.25 | 39.6 | −0.2 | −0.09 | – | – | @298 K | ("OLI Stream Analyser 3.2") |
| $CaCl_2$ | 8.51 | 50.95 | 20.66 | 4.52 | −0.5 | – | – | @298 K | ("OLI Stream Analyser 3.2") |
| Glucose | $\pi = 101325 \times 0.0821 \times T(K) \times C$(Van't Hoff's equation) | | | | | | | For dilute solution | – |

## References


Abramowitz, M., Stegun, I.A., 1964. Handbook of Mathematical Functions: With Formulas, Graphs, and Mathematical Tables. Courier Corporation.

Achilli, A., Cath, T.Y., Marchand, E.A., Childress, A.E., 2009. The forward osmosis membrane bioreactor: a low fouling alternative to MBR processes. Desalination 239, 10–21.

Alnouri, S.Y., Linke, P., El-Halwagi, M.M., 2016. Synthesis of industrial park water reuse networks considering treatment systems and merged connectivity options. Comput. Chem. Eng. 91, 289–306.

Bonabeau, E., 2002. Agent-based modeling: methods and techniques for simulating human systems. PNAS 99, 7280–7287.

Borsi, I., Lorain, O., 2012. A space-averaged model for hollow fibre membranes filters. Comput. Chem. Eng. 39, 65–74.

Bui, A.V., Nguyen, M., 2004. Prediction of viscosity of glucose and calcium chloride solutions. J. Food Eng. 62, 345–349.

Castaldi, M., D'Errico, G., Paduano, L., Vitagliano, V., 1998. Transport properties of the binary system glucose-water at 25 °C: A velocity correlation study. J. Chem. Eng. Data 43, 653–657.

Cath, T.Y., Childress, A.E., Elimelech, M., 2006. Forward osmosis: principles, applications, and recent developments. J. Membr. Sci. 281, 70–87.

Chung, T.-S., Li, X., Ong, R.C., Ge, Q., Wang, H., Han, G., 2012. Emerging forward osmosis (FO) technologies and challenges ahead for clean water and clean energy applications. Curr. Opin. Chem. Eng. 1, 246–257.

Dabaghian, Z., Rahimpour, A., 2015. Carboxylated carbon nanofibers as hydrophilic porous material to modification of cellulosic membranes for forward osmosis desalination. Chem. Eng. Res. Des. 104, 647–657.

Damaceanu, R.-C., 2008. An agent-based computational study of wealth distribution in function of resource growth interval using NetLogo. Appl. Math. Comput. 201, 371–377.

Deshmukh, A., Yip, N.Y., Lin, S., Elimelech, M., 2015. Desalination by forward osmosis: identifying performance limiting parameters through module-scale modeling. J. Membr. Sci. 491, 159–167.

Elimelech, M., 2006. The global challenge for adequate and safe water. J. Water Supply Res. Technol. AQUA 55, 3–10.

Eo, S.Y., Chang, T.S., Shin, D., Yoon, E.S., 2000. Cooperative problem solving in diagnostic agents for chemical processes. Comput. Chem. Eng. 24, 729–734.

Geraldes, V.T., Semião, V., de Pinho, M.N., 2001. Flow and mass transfer modelling of nanofiltration. J. Membr. Sci. 191, 109–128.

Grosman, P.D., Jaeger, J.A., Biron, P.M., Dussault, C., Ouellet, J.-P., 2011. Trade-off between road avoidance and attraction by roadside salt pools in moose: an agent-based model to assess measures for reducing moose-vehicle collisions. Ecol. Modell. 222, 1423–1435.

Gruber, M., Johnson, C., Tang, C., Jensen, M.H., Yde, L., Hélix-Nielsen, C., 2011. Computational fluid dynamics simulations of flow and concentration polarization in forward osmosis membrane systems. J. Membr. Sci. 379, 488–495.

Gruber, M.F., Aslak, U., Hélix-Nielsen, C., 2016. Open-source CFD model for optimization of forward osmosis and reverse osmosis membrane modules. Sep. Purif. Technol. 158, 183–192.

Jiao, B., Cassano, A., Drioli, E., 2004. Recent advances on membrane processes for the concentration of fruit juices: a review. J. Food Eng. 63, 303–324.

Juang, R.-S., Kao, H.-C., Tseng, K.-J., 2010. Kinetics of phenol removal from saline solutions by solvent extraction coupled with degradation in a two-phase partitioning bioreactor. Sep. Purif. Technol. 71, 285–292.

Jung, D.H., Lee, J., Lee, Y.G., Park, M., Lee, S., Yang, D.R., Kim, J.H., 2011. Simulation of forward osmosis membrane process: effect of membrane orientation and flow direction of feed and draw solutions. Desalination 277, 83–91.

Katare, S., Venkatasubramanian, V., 2001. An agent-based learning framework for modeling microbial growth. Eng. Appl. Artif. Intell. 14, 715–726.

Kumar, R., Pal, P., 2015. A novel forward osmosis-nano filtration integrated system for coke-oven wastewater reclamation. Chem. Eng. Res. Des. 100, 542–553.

Laliberté, M., 2007. Model for calculating the viscosity of aqueous solutions. J. Chem. Eng. Data 52, 321–335.

Li, W., Gao, Y., Tang, C.Y., 2011. Network modeling for studying the effect of support structure on internal concentration polarization during forward osmosis: model development and theoretical analysis with FEM. J. Membr. Sci. 379, 307–321.

Lutchmiah, K., Verliefde, A., Roest, K., Rietveld, L.C., Cornelissen, E.R., 2014. Forward osmosis for application in wastewater treatment: a review. Water Res. 58, 179–197.

Macal, C.M., North, M.J., 2010. Tutorial on agent-based modelling and simulation. J. Simul. 4, 151–162.

Mahmoodi, N.M., Chamani, H., Kariminia, H.-R., 2016. Functionalized copper oxide–zinc oxide nanocomposite: synthesis and genetic programming model of dye adsorption. Desalin. Water Treat. 57, 18755–18769.

Mansury, Y., Deisboeck, T.S., 2004. Simulating the time series of a selected gene expression profile in an agent-based tumor model. Phys. D 196, 193–204.

McCutcheon, J.R., Elimelech, M., 2006. Influence of concentrative and dilutive internal concentration polarization on flux behavior in forward osmosis. J. Membr. Sci. 284, 237–247.

McCutcheon, J.R., Elimelech, M., 2007. Modeling water flux in forward osmosis: implications for improved membrane design. AIChE J. 53, 1736–1744.
McCutcheon, J.R., McGinnis, R.L., Elimelech, M., 2005. A novel ammonia—carbon dioxide forward (direct) osmosis desalination process. Desalination 174, 1–11.
McCutcheon, J.R., McGinnis, R.L., Elimelech, M., 2006. Desalination by ammonia–carbon dioxide forward osmosis: influence of draw and feed solution concentrations on process performance. J. Membr. Sci. 278, 114–123.
Miller, D.G., Rard, J.A., Eppstein, L.B., Albright, J.G., 1984. Mutual diffusion coefficients and ionic transport coefficients lij of magnesium chloride-water at 25 °C. J. Phys. Chem. 88, 5739–5748.
OLI Stream Analyser 3.2, OLI Systems Inc., Morris Plains, NJ,US. http://www.olisystems.com/.
Pardeshi, P.M., Mungray, A.A., Mungray, A.K., 2016. Determination of optimum conditions in forward osmosis using a combined Taguchi–neural approach. Chem. Eng. Res. Des. 109, 215–225.
Paton, R., Gregory, R., Vlachos, C., Saunders, J., Wu, H., 2004. Evolvable social agents for bacterial systems modeling. IEEE Trans. Nanobiosci. 3, 208–216.
Phuntsho, S., Vigneswaran, S., Kandasamy, J., Hong, S., Lee, S., Shon, H.K., 2012. Influence of temperature and temperature difference in the performance of forward osmosis desalination process. J. Membr. Sci. 415, 734–744.
Phuntsho, S., Hong, S., Elimelech, M., Shon, H.K., 2014. Osmotic equilibrium in the forward osmosis process: modelling, experiments and implications for process performance. J. Membr. Sci. 453, 240–252.
Pogson, M., Smallwood, R., Qwarnstrom, E., Holcombe, M., 2006. Formal agent-based modelling of intracellular chemical interactions. Biosystems 85, 37–45.
Railsback, S.F., Lytinen, S.L., Jackson, S.K., 2006. Agent-based simulation platforms: review and development recommendations. Simulation 82, 609–623.
Rard, J.A., Miller, D.G., 1979a. The mutual diffusion coefficients of Na2SO4-H2O and MgSO4- H2O at 25 °C from Rayleigh interferometry. J. Solution Chem. 8, 755–766.
Rard, J.A., Miller, D.G., 1979b. The mutual diffusion coefficients of NaCl-H2O and CaCl2-H2O at 25 °C from Rayleigh interferometry. J. Solution Chem. 8, 701–716.
Sagiv, A., Semiat, R., 2011. Finite element analysis of forward osmosis process using NaCl solutions. J. Membr. Sci. 379, 86–96.
Sagiv, A., Zhu, A., Christofides, P.D., Cohen, Y., Semiat, R., 2014. Analysis of forward osmosis desalination via two-dimensional FEM model. J. Membr. Sci. 464, 161–172.
Shim, S.-M., Kim, W.-S., 2013. A numerical study on the performance prediction of forward osmosis process. J. Mech. Sci. Technol. 27, 1179–1189.
Soni, V., Abildskov, J., Jonsson, G., Gani, R., 2009. A general model for membrane-based separation processes. Comput. Chem. Eng. 33, 644–659.
Tan, C.H., Ng, H.Y., 2008. Modified models to predict flux behavior in forward osmosis in consideration of external and internal concentration polarizations. J. Membr. Sci. 324, 209–219.
Tang, C.Y., She, Q., Lay, W.C., Wang, R., Fane, A.G., 2010. Coupled effects of internal concentration polarization and fouling on flux behavior of forward osmosis membranes during humic acid filtration. J. Membr. Sci. 354, 123–133.
Thorsen, T., Holt, T., 2009. The potential for power production from salinity gradients by pressure retarded osmosis. J. Membr. Sci. 335, 103–110.
UNESCO 2011. The United Nations world water development report.
Van Dam, K.H., Adhitya, A., Srinivasan, R., Lukszo, Z., 2008. Benchmarking numerical and agent-based models of an oil refinery supply chain. Comput. Aided Chem. Eng. 25, 623–628.
Wilensky, U., 1999. Netlogo (and Netlogo User Manual). Center for Connected Learning and Computer-Based Modeling, Northwestern University http://ccl.northwestern.edu/netlogo/.
Yang, Q., Wang, K.Y., Chung, T.-S., 2009. A novel dual-layer forward osmosis membrane for protein enrichment and concentration. Sep. Purif. Technol. 69, 269–274.